

Excited state vibrational dynamics of 4-ethylaniline (X)₁ clusters (X=Ar, N₂, and CH₄)

Max F. Hineman, Elliot R. Bernstein, and David F. Kelley

Citation: *The Journal of Chemical Physics* **98**, 2516 (1993); doi: 10.1063/1.464187

View online: <http://dx.doi.org/10.1063/1.464187>

View Table of Contents: <http://aip.scitation.org/toc/jcp/98/4>

Published by the *American Institute of Physics*

COMPLETELY

REDESIGNED!



**PHYSICS
TODAY**

Physics Today Buyer's Guide
Search with a purpose.

Excited state vibrational dynamics of 4-ethylaniline (X)₁ clusters (X=Ar, N₂, and CH₄)

Max F. Hineman, Elliot R. Bernstein, and David F. Kelley
Colorado State University, Department of Chemistry, Fort Collins, Colorado 80523

(Received 15 September 1992; accepted 27 October 1992)

Intracluster vibrational redistribution (IVR) and vibrational predissociation (VP) dynamics of 4-ethylaniline (Ar)₁, (N₂)₁, and (CH₄)₁ clusters have been studied by time-correlated single photon counting, mass-resolved excitation spectroscopy, and dispersed emission spectroscopy. The 4-ethylaniline molecule has a low frequency ethyl group torsion vibrational mode, which is similar in energy to the van der Waals modes of the clusters. This mode, because of its low energy (~ 35 cm⁻¹), plays a role in the vibrational dynamics of the clusters studied. The cluster dissociation rates and product state distributions can be modeled by a serial IVR/VP mechanism for which the VP step is treated by the Rice–Ramsperger–Kassel–Marcus (RRKM) theory. The resulting agreement between the calculated and experimental rates and product state intensities indicates that a statistical distribution of energy among all low frequency modes exists for 4-ethylaniline/polyatomic solvent clusters in which $k_{\text{IVR}} \gg k_{\text{VP}}$. For 4-ethylaniline (Ar)₁ clusters $k_{\text{VP}} > k_{\text{IVR}}$ and a statistical distribution of energy among the chromophore and van der Waals modes is not achieved. The central determining factor for the vibrational dynamics of these clusters is overall density of low energy modes.

I. INTRODUCTION

One of the central questions addressed in the study of intramolecular (cluster) vibrational energy redistribution (IVR) and vibrational predissociation (VP) in polyatomic van der Waals clusters¹⁻⁵ has been, “Is the IVR/VP process mode specific; i.e., are certain product vibrational states selectively populated?” While this question has been addressed by both static and dynamic spectroscopic studies, in many cases its answer is critically dependent on the assumed model for the IVR/VP process.

Most early treatments of IVR and VP in van der Waals clusters consider these two processes in terms of a parallel model; i.e., IVR and VP occur together independently.¹ In such a model, all final product (bare molecule) vibrational states result directly from VP of the initial photoexcited cluster vibrational state. Within the framework of this model, mode selectivity is immediately obvious. All energetically accessible bare molecule states should be populated and deviation from this prediction is taken to be an example of nonstatistical mode selectivity.

We have suggested that the dynamical behavior of vibrationally excited van der Waals clusters is not quite so simple,^{3(c)} and that IVR and VP are serial processes. Energy must first flow from the high frequency chromophore modes into the low frequency van der Waals modes (IVR). Once sufficient energy is in these low frequency, strongly coupled modes, the VP process is statistical, just as it would be in any other unimolecular dissociation reaction for which a very high density of vibrational states is present in the molecule. The VP rate constant may then be calculated by the Rice–Ramsperger–Kassel–Marcus (RRKM) theory.^{3(c)}

An essential and tacit assumption of this model is that the VP process itself has no effect on the chromophore vibrational state. In this sense, dissociation is considered to

be vibrationally adiabatic. This model is complicated by the fact that VP may compete with subsequent energy flow into the vibrational phase space of the van der Waals modes. Such flow results in VP rates which vary as IVR proceeds. Under these circumstances, terms such as “nonstatistical” must be carefully defined. IVR rates depend on the couplings between vibrational states and as such are inherently nonstatistical. Thereby, even if the VP rates for any specified amount of energy in the van der Waals modes are indeed given by RRKM theory, a complicated distribution of final product states may obtain. This distribution might then be interpreted as “nonstatistical” or “mode-specific” VP; however, because the VP rates are given by RRKM theory we would consider this point of view to be incorrect.

One special case of the serial IVR/VP model which is commonly encountered involves clusters for which IVR is much faster than VP. In these cases, all VP rates may be calculated from statistical theories ignoring the IVR process completely. For example, this was found to be the case for aniline (CH₄)₁.^{3(a)}

Throughout the previous studies of IVR/VP processes, the cluster vibrational phase space has been separated into two distinct regions—the high frequency chromophore modes and the low frequency van der Waals modes. When this is the case, virtually the entire contribution to the total density of vibrational states comes from the van der Waals modes. Thus, in the absence of VP, IVR results in the almost complete and irreversible flow of energy from the chromophore to the van der Waals modes.

In this paper, we explore the dynamical consequences of low frequency chromophore modes. This is accomplished by studying van der Waals complexes of “ring-tail” aromatic molecules, specifically alkylanilines.

Ring-tail systems⁴⁻⁸ alkylbenzenes and alkylanilines play an important role in the elucidation of IVR in isolated

molecule systems. The addition of an alkyl chain to the aromatic ring molecules typically used to study IVR adds several low frequency modes to the vibrational phase space. These additional modes significantly increase the vibrational density of states and thereby affect the rates of IVR. The effect of these low frequency chromophore modes on the IVR/VP processes in clusters has not been fully explored.⁸ The questions which one might ask about these cluster systems include does the IVR behavior of the cluster favor chromophore mode to chromophore mode IVR when the lowest frequency chromophore vibrations are of similar energy to the van der Waals modes of the cluster; does the addition of low frequency chromophore vibrations to the vibrational phase space of the cluster alter the VP rates; and can the final product distribution of chromophore state be described by statistical theories? In order to address these questions, we have studied the nanosecond and picosecond time-resolved fluorescence spectra of a series of clusters of 4-ethylaniline (4EA): 4EA(Ar)₁; 4EA(N₂)₁; and 4EA(CH₄)₁. 4EA is one of the ring-tail IVR systems previously studied as an isolated molecule.⁴⁻⁸ We find that while the results might be interpreted as being highly mode specific, they can be modeled quantitatively by simple RRKM theory.

II. PROCEDURES

A. Experiment

The vibrational dynamics of the excited clusters are studied by time-correlated, single photon counting (TC-SPC). The experimental apparatus has been described previously.^{3(a)} The system consists of a cavity dumped, frequency doubled, rhodamine 575 dye laser synchronously pumped by a mode-locked cw Nd:YAG laser. The output of the dye laser consists of frequency tunable ultraviolet radiation of ~ 5 – 10 ps pulses (4 MHz repetition rate) and average power of ~ 10 mW. A cw molecular jet is used as the cluster source—the molecular beam and laser beam intersect at 90° . The instrument response function for the system is measured prior to each experiment by two methods—scattering of laser light into the emission monochromator, and fitting of the rise of a zero rise time emission signal which has a long decay time relative to the instrument response (e.g., excite 4EA 0_0^0 , observe I_2^0). The instrument response function is typically ~ 200 ps with the monochromator set in the first order of a 2400 grooves/mm grating.

Mass-resolved excitation spectra are obtained using a two-color, resonance-enhanced, two-photon ionization technique with time-of-flight mass detection. The apparatus used for these experiments is quite standard and has been described previously.⁹

The 4-ethylaniline was inserted into the nozzle in a sample boat and the nozzle was heated to $\sim 30^\circ\text{C}$. The driving gas is 50 psig of He for bare molecule measurements and 50 psig of 1% Ar, 1% CH₄, and 0.7% N₂ in He for Ar, CH₄, and N₂ cluster studies, respectively.

B. Calculation

Calculation of VP rates using RRKM theory for unimolecular reactions requires the value of sums and densities of states.^{3(c)} Specifically, the density of vibrational states at the excitation energy and the sum of vibrational states, omitting the reaction coordinate, at the excess energy (energy greater than the binding energy of the cluster) are required. The “semiclassical” (e.g., Marcus–Rice) approximations to these quantities are inaccurate at low energies ($E < 300\text{ cm}^{-1}$). These quantities can be calculated using direct count methods at low energies. van der Waals mode energies are calculated by a normal mode analysis of the cluster performed using an atom–atom potential for van der Waals force constant calculations.^{10,11} An exponential-6 potential is used to calculate the cluster structures and van der Waals modes energies.¹² This potential includes Coulomb interactions for the partial charges on the atomic centers of the solute and solvent molecules. 4EA and aniline partial charges are obtained by fitting the electric field of the molecule, calculated by *ab initio* quantum mechanical methods (HONDO-8)¹³ to partial charges on the atomic centers.¹¹ The comparison with aniline serves as verification of the accuracy of the calculations. The quadrupole moment of the nitrogen molecule is modeled by placing additional point charges 0.25 \AA away from each nitrogen atom.¹¹

III. RESULTS

A. 4-ethylaniline

The excitation spectrum of 4-ethylaniline has been published previously.⁶ The origin is allowed and vibronic features are observed at 84, 435 ($6a^1$), 739 (I^2), and 810 cm^{-1} (1^1) above the 0_0^0 transition. Weak hot bands at -12 and -24 cm^{-1} are also observed in the mass-resolved excitation spectrum. The 84 cm^{-1} peak and the 12 cm^{-1} hot band sequence structure have not been assigned previously.

Since low energy modes of 4EA will be important for the 4EA cluster vibrational dynamics, we must consider the nature of both the 84 cm^{-1} feature and the 12 cm^{-1} sequence difference. The 84 cm^{-1} excited electronic state mode appears paired in terms of intensity and Franck–Condon factor with a 100 cm^{-1} mode in the ground state based on both excitation and dispersed emission spectra. Thus the -12 cm^{-1} sequence structure is not related to this mode pair, but rather a mode of lower energy. We do not observe any other hot band structure for this system and mode selective cooling or noncooling in the expansion process seems unlikely. Thus the -12 cm^{-1} sequence structure is caused by a lower energy mode than the 84 cm^{-1} mode whose excited electronic state energy is smaller than its ground electronic state energy by 12 cm^{-1} .

The two possible modes that can contribute to the low energy vibrational space of 4EA are the ethyl bend in the plane of the molecule (containing heavy atoms NC₁C₄C₇C₈) and the ethyl torsion perpendicular to the plane of the molecule.

The $84/100\text{ cm}^{-1}$ mode might also be due to an overtone of a nontotally symmetric lower energy mode ($42/50$

TABLE I. Spectral shifts of $S_1 \leftarrow S_0$ electronic transition for aniline and 4EA clusters. All units are cm^{-1} .

Solute/solvent	Ar	CH ₄	N ₂
Aniline	53	77	125
4-ethylaniline	57	87	140

cm^{-1}) such as the torsion. Three different arguments suggest this latter possibility is not correct. First, the assignment of the 84/100 cm^{-1} bands as overtones leads to the following contradiction: the Franck–Condon factor for the transition to an undisplaced overtone of an oscillator is too small to account for the observed intensity. Displacement of the oscillator can dramatically increase this Franck–Condon factor; however, the torsional displacement would reduce the excited state to C_1 symmetry and cause the fundamental to become allowed. No feature in either the hot or cold spectrum of 4EA suggests a 42/50 cm^{-1} pair of modes. Second, semiempirical (MOPAC 6)¹⁴ calculations of the ground state vibrations of 4EA give the torsion at 34 cm^{-1} and the bend at 98 cm^{-1} . Consistent with these calculations, the torsion for 3EA is assigned at 45 cm^{-1} .¹⁵ Third, the deuterium isotope effect on the 84 cm^{-1} feature is consistent with the bending mode rather than the torsional mode. The isotope effect on the torsional mode energy is calculated to be less than 1% for amino- d_2 substitution, while the isotope effect on the bending mode energy is calculated to be 3% for the same substitution. The feature in question shifts from 84.6 cm^{-1} for amino- h_2 4EA to 81.7 cm^{-1} for amino- d_2 4EA—a change of 3.4%. Thus, the 84/100 cm^{-1} mode pair of 4EA is assigned as the totally symmetric bending mode of the ethyl group.

The most plausible assignment of the 12 cm^{-1} hot band progression is to the ethyl torsion. Assignment of the ethyl bend is eliminated because the ground to excited state energy difference is 16 cm^{-1} , as determined from the 84 cm^{-1} peak in the excitation spectrum and 100 cm^{-1} peak in the dispersed emission spectrum. Also, the ethyl torsion is calculated to be the lowest frequency mode and is thus most likely to exhibit hot bands. This 12 cm^{-1} progression, however, tells us neither the ground nor excited state frequencies, just the difference between the two. One can expect that the torsion would have an energy of roughly 30–40 cm^{-1} based on calculation and the 3EA data.

B. Clusters

Mass-resolved excitation spectra of the clusters show red shifted origins and vibrations as well as red shifted ionization potentials relative to those of bare 4EA. Table I lists the spectroscopic shifts of the $S_1 \leftarrow S_0$ origins for the Ar, CH₄, and N₂ clusters. The red shifts indicate an increase in cluster binding energy in the excited state. The 4EA cluster shifts are larger than the comparable aniline cluster shifts. This implies that the binding energy difference (ground to excited state) is greater for the 4EA clusters and, as discussed below, that the binding energies

DE SPECTRA OF 4EA(Ar)₁

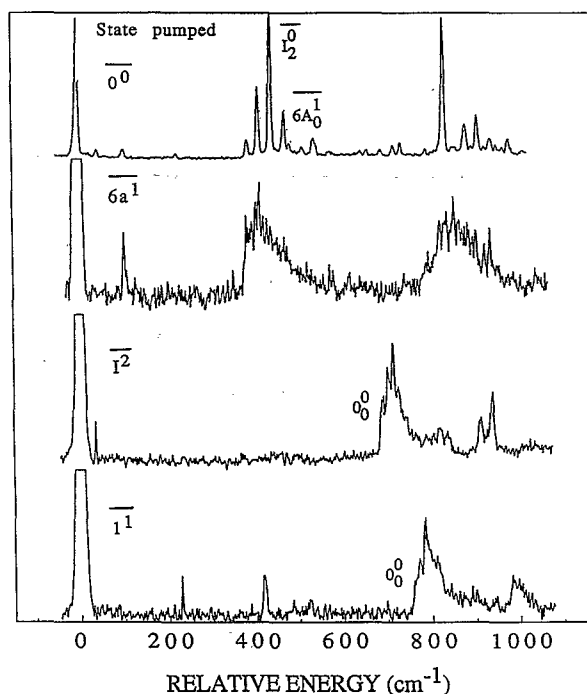


FIG. 1. Dispersed emission spectra of 4EA(Ar)₁ clusters arising from various excited cluster states. Positive numbers indicate the red shift from the excitation wavelength.

themselves are slightly larger for the 4EA clusters than for the aniline cluster.

The binding of the solvent species is primarily to the benzene ring as no hydrogen bonding is expected for these systems. In this case and given the structure of 4EA (the ethyl group perpendicular to the plane of the ring), one would expect two possible conformations for each one to one cluster—one conformation with the solvent on the same side of the ring as the ethyl group and the other with the solvent on the opposite side of the ring from the ethyl group. These two structures are calculated, by the atom-atom potentials described above, to have 50 (Ar) and 90 cm^{-1} (N₂ and CH₄) differences in binding energy. In this case, given the calculated 170 cm^{-1} barrier to rotation of the ethyl group, one might well expect to see spectra associated with both conformations for each cluster; however, no evidence for multiple conformation in either the excitation or emission spectra of these clusters can be identified. The cluster formation process may be slow enough in this case that only the lower energy conformation of the clusters, with the solvent molecules on the same side of the ring as the ethyl moiety, survive in the cold form.

Dispersed emission spectra of the bare molecule have been published.⁶ Dispersed emission spectra of the 4EA(Ar)₁ cluster are shown in Fig. 1. The dispersed emission spectrum following origin excitation is virtually identical to the bare molecule emission spectrum with the addition of very weak van der Waals mode peaks.

Following $6a^1$ (the bar indicates a cluster state or tran-

sition) excitation, the $4EA(Ar)_1$ emission spectrum is broad and quite similar to those found for aniline $(N_2)_1$ and aniline $(CH_4)_1$ clusters.³ These broad spectra indicate that the cluster is left with significant excitation in the van der Waals and probably the low frequency chromophore vibrations. Because the spectra are congested, the various low energy states of the $4EA$ molecule which may be populated cannot be identified. The absence of bare molecule emission following $6a^1$ (435 cm^{-1}) excitation suggests that no VP occurs at this energy. This is not surprising as the $6a^1$ vibration for $4EA$ is considerably lower in energy (435 cm^{-1}) than the $6a^1$ vibration of aniline (494 cm^{-1}) and the binding energies of the $4EA$ clusters are expected to be larger. At 435 cm^{-1} , the aniline clusters would not be expected to dissociate. The dispersed emission spectra following $6a^1$ excitation for $4EA(N_2)_1$ and $(CH_4)_1$ clusters show the same broad emission as the Ar cluster.

The emission following \bar{I}^2 and \bar{I}^1 excitation is, however, quite different for the different clusters. Figure 2 shows the emission of the various clusters near the bare molecule origin following \bar{I}^2 and \bar{I}^1 excitation. The resolution of the spectra shown in Fig. 2 is $\sim 2.5\text{ cm}^{-1}$. Bare molecule emission dominates the observed spectra with little evidence of cluster emission.

The N_2 and CH_4 clusters emit only from a sequence of peaks each shifted successively 12 cm^{-1} to the red of the bare molecule origin. The number of members in the sequence increases with excitation energy (see Fig. 2) and is affected by cluster solvent (fewer members for N_2 than CH_4). The sequence structure is the same for all four polyatomic solvent emissions—the bare molecule 0_0^0 is the most intense feature of this sequence and the sequence of 12 cm^{-1} red shifted peak intensities decreases monotonically. We assign this sequence to $\Delta v=0$ hot emission from the low frequency ethyl torsion mode of the bare molecule. In order to populate this mode in the high vibrational levels observed ($v=4$ following \bar{I}^1 excitation), the mode energy must be below about 100 cm^{-1} . In fact, the mode energy is probably considerably lower than 100 cm^{-1} since that would require almost all of the excess energy to be deposited in this mode. Note that a 12 cm^{-1} , but no 16 cm^{-1} progression is observed in the $4EA(N_2)_1$ and $4EA(CH_4)_1$ emission spectra and that a 12 cm^{-1} hot band sequence is observed for the $4EA$ bare molecule. A 16 cm^{-1} sequence structure would arise if the 84 cm^{-1} (S_1)/ 100 cm^{-1} (S_0) ethyl bending mode were involved in the observed transitions.

Following \bar{I}^2 and \bar{I}^1 excitation of the $4EA(Ar)_1$ cluster, two members of the 12 cm^{-1} sequence and another sequence in 12 cm^{-1} built on a 16 cm^{-1} feature can be identified, as well as other reproducible peaks which remain unassigned. In this instance, the spectrum is crowded and overlapped making relative intensity measurements difficult.

Time-resolved studies (TCSPC) following excitation of the clusters and bare solute molecule to various vibrational states are also carried out. Figure 3 shows a typical fit of an experimental decay curve. The results of the decay

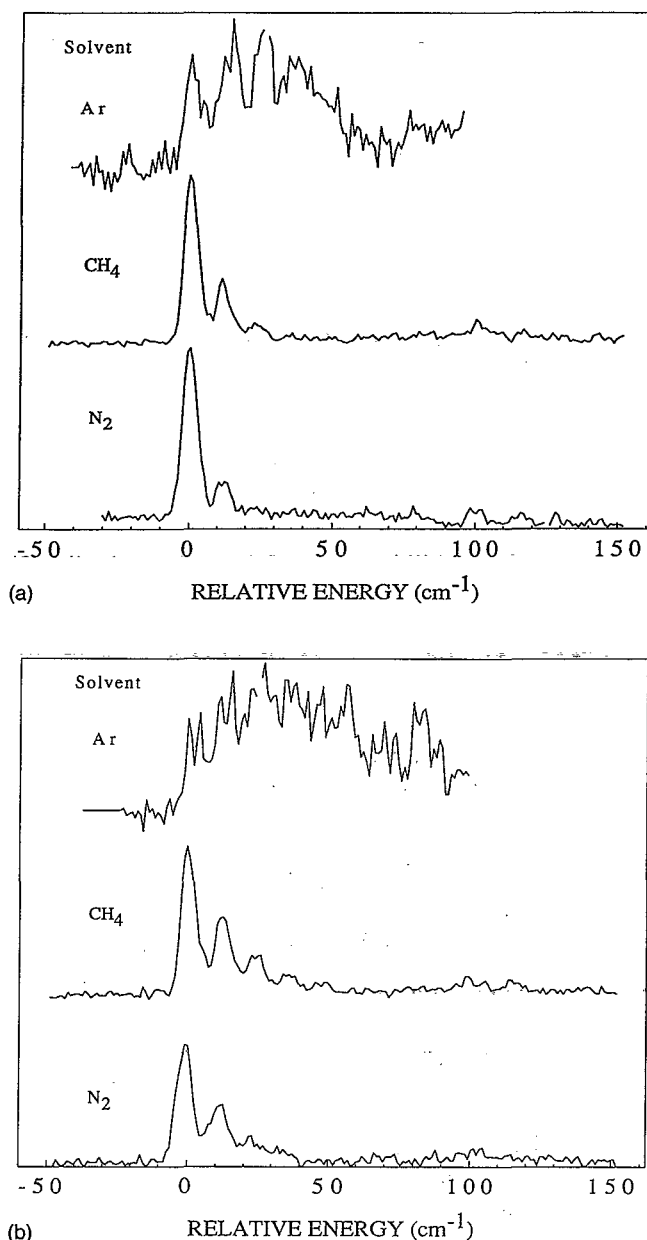


FIG. 2. Dispersed emission spectra of $4EA(\text{solvent})_1$ clusters expanded near the $4EA$ origin region. (a) \bar{I}^2 excitation; (b) \bar{I}^1 excitation. Positive numbers indicate a red shift from the $4EA$ bare molecule origin.

curve fits are collected in Table II. Decay curves for the bare $4EA$ molecule show that IVR among the chromophore modes starts to occur at vibrational levels as low as $6a^1$ for the monomer (identified through biexponential decays). Observation of IVR at such low excitation energy above 0_0^0 shows the strong effect of the low frequency vibrations on the IVR rates of ring-tail molecules.

The rise time of the broad features near the cluster origin following $6a^1$ excitation gives the total IVR rate into the van der Waals modes since no VP occurs at this vibrational energy. The increasing number of van der Waals modes for the cluster series Ar , N_2 , and CH_4 increases the van der Waals mode density of states and would therefore be expected to give rise to a decreasing rise time and in-

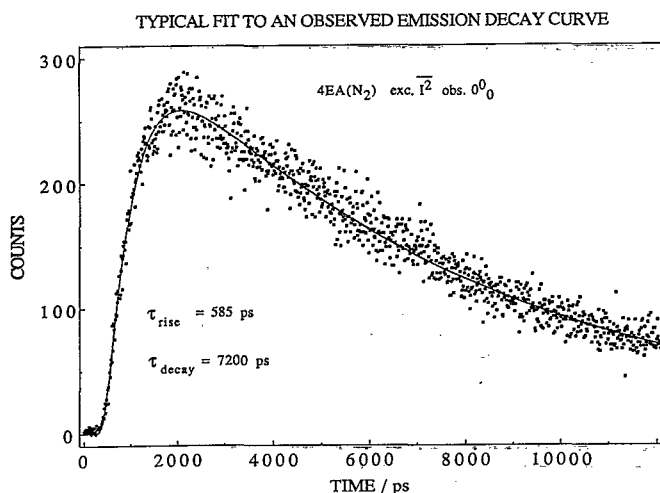


FIG. 3. A typical fit of an observed TCSPC decay curve. Data correspond to the $4EA(N_2)_1$ cluster pumped at \bar{I}^2 and observed at 0_0^0 . The fit parameters are rise time 585 ps and decay time 7200 ps.

creasing IVR rate. This trend is observed to the extent that such times can be measured. Given the instrument response function of ~ 200 ps, the rise times for this emission ($6a^1$ excitation— 0_0^0 observation) cannot be resolved for the N_2 and CH_4 clusters.

The rise time of the bare 4EA origin features following \bar{I}^2 and \bar{I}^1 excitation gives the sum of the IVR and VP times. Based on the $6a^1$ excitation results and the high vibrational energy and concomitant high density of states at these energies, IVR should be very fast for $4EA(N_2)_1$ and $(CH_4)_1$ clusters. No emission is observed from the pumped states \bar{I}^2 and \bar{I}^1 states in agreement with this expectation. Thus the measured 0_0^0 bare molecule rise times for these clusters at higher vibrational excitation should correspond to the VP time.

Calculated van der Waals mode energies and binding energies are given in Table III. Binding energies for $4EA(Ar)_1$ and $(CH_4)_1$ clusters are well fit; the calculated binding energy for the $4EA(N_2)_1$ cluster is $\sim 15\%$ too high. The "experimental" binding energies presented in Table III are derived by fitting the kinetic data and are

TABLE II. Results of fitting decay curves for 4-ethylaniline clusters.

State pumped	Transition observed	Solvent	Rise time (ps)	Decay time (ps)
$6a^1$	0_0^0	Ar	200	6000
		CH_4	<100	6200
		N_2	80	6900
\bar{I}^2	0_0^0	Ar	250	8200
		CH_4	400	8000
		N_2	585	7200
\bar{I}^1	0_0^0	Ar	185	7200
		CH_4	110	8000
		N_2	125	7200

discussed below. The sensitivity of the RRKM calculated VP rates to van der Waals mode energies and anharmonicities will be elaborated in the Discussion section.

IV. DATA ANALYSIS—RRKM THEORY

The data presented in the Results section show features of the IVR/VP process which any theory of van der Waals molecule dissociation must be able to reproduce. First, only the bare molecule ethyl torsion mode and 0_0^0 are populated and emit following IVR and VP of $4EA/polyatomic$ solvent clusters. Second, specific product state distributions in the torsional mode manifold are observed which depend on the cluster and the excitation energy. Third, the rate of dissociation depends on the excitation energy. Fourth, the emission behavior of the three clusters studied is qualitatively different from each other. To this end, we have applied the RRKM theory of unimolecular reactions to the calculation of the numerical data for N_2 and CH_4 clusters as well as qualitative evaluation of the Ar cluster results.

The model we employ to understand the results presented in the last section consists of the following conditions and assumptions: First, IVR/VP are serial processes. IVR occurs first from the excited chromophore modes to the van der Waals modes. Only after the van der Waals modes are populated with sufficient energy will the cluster undergo VP. Second, the rate of dissociation is given by the RRKM theory once the van der Waals modes have sufficient energy to cause dissociation. If we consider the case for which all IVR is rapid ($4EA/polyatomic$ clusters) compared to VP, then the vibrational energy in the cluster is partitioned statistically among the chromophore and van der Waals modes. This latter approximation results in considerable simplification of the model. Dissociation may occur whenever the amount of energy in the van der Waals modes exceeds the cluster binding energy and the rate of dissociation is then given by the RRKM theory. When the excited clusters dissociate from a given cluster vibrational state, the energy which was (statistically) proportioned into chromophore vibrational modes remains in the bare chromophore molecule after dissociation. These states of the bare chromophore then fluoresce with their characteristic emission wavelengths and times. The relative intensities of these emissions give the population distribution within the manifold of bare 4EA states. These bare solute distributions can then be related to the cluster state distributions and rates of dissociation.

Based on previous results from this laboratory on aniline/Ar, N_2 , and CH_4 clusters,^{3(a),3(b)} the IVR rate among the low frequency modes of 4EA clusters should be very high.^{3(c)} Given this rapid flow of energy among the low frequency modes of the cluster, an equilibrium among all of these modes should exist. In this case, the intensity of a product state (bare molecule) emission will be given by the rate of dissociation from the parent cluster state multiplied by the probability of populating that cluster state $P_j k(v)$.

The RRKM theory of unimolecular reactions predicts that the rate constant for dissociation will be given by^{3(c)}

TABLE III. Results of cluster van der Waals normal mode analysis—calculated van der Waals frequencies and binding energy. All units are cm^{-1} . Experimental (fit) binding energies in parentheses.

Solvent/solute	Aniline		4-ethylaniline	
	vdW modes	Binding energy	vdW modes	Binding energy
Ar	42, 24, 16	415 (450)	43, 25, 24	535 (···)
CH ₄	116, 59, 55, 38, 26, 13	464 (480)	76, 72, 63, 48, 28, 3	582 (580)
N ₂	75, 60, 31, 25, 20	596 (515)	79, 59, 33, 26, 16	723 (630)

$$k_v = (1/h) \sum P(E^+) / N(E - E_v) \quad (1)$$

in which E is the total cluster vibrational energy, E_v is the amount of energy in the chromophore vibrations, and $N(E - E_v)$ is the density of states at the (vibrational) excitation energy minus the energy restricted to the chromophore vibrations. $\sum P(E^+)$ is the sum of states above the dissociation energy, not including the reaction coordinate; i.e., $E^+ = E - E_v - E_0$ (E_0 is the binding energy of the cluster).

The probability of populating a state with energy E_v restricted into the chromophore vibrations is proportional to the ratio of the density of van der Waals states at $E - E_v$ to that at E ,¹⁶

$$P_v = [N(E - E_v) / N(E)] / \sum_v [N(E - E_v) / N(E)] \quad (2)$$

in which $N(E)$ is the density of states at energy E . Assuming that the Franck-Condon factors for all $\Delta v = 0$ transitions within the torsional mode manifold are equal, the relative intensities of product state emissions will be the rate of dissociation of the cluster state multiplied by the probability of populating that state

$$I(v) = P_v k(v). \quad (3)$$

The total dissociation rate from these equilibrated modes will be given by the sum of the rates out of each state multiplied by the probability of populating each state¹⁶

$$k(E) = \sum_v P_v k(v). \quad (4)$$

This is of course equal to the RRKM rate obtained by considering all the vibrational (chromophore + van der Waals) modes

$$k(E) = (1/h) P(E - E_0) / N(E).$$

Evaluation of Eqs. (1) and (3) requires the calculation of the sums and densities of van der Waals vibrational states. These are calculated by a direct count method,¹⁷ which requires values of the vibrational frequencies. Since Eq. (1) is restricted to the van der Waals modes, only these frequencies are required. The low frequency chromophore modes which are populated by the IVR/VP processes are not part of this count because the rates for each of the states of these vibrations will be calculated individually and thus the energy in these modes will be restricted or isolated in the calculation. As discussed above, the van der Waals mode energies are calculated using an atom-atom potential model and normal mode analysis. The density of states is a strongly nonmonotonic function of energy at low energies. It is characterized by peaks and valleys, the energies of which are strongly dependent on the as-

sumed frequencies. Thus, at low energies (below 100 cm^{-1}), the required sums and densities are not well calculated by these methods due to inadequacies in both the model potential and the harmonic approximation. Nonetheless, because the RRKM rates are a function of a sum of states divided by a density of states, a significant amount of cancellation of these errors is to be expected. The calculated van der Waals mode energies are listed in Table III. A sensitivity analysis is done to test the effect of mode energies on the calculated rates and product state distributions and will be discussed below.

To complete the RRKM calculations for the cluster dissociation rates and final bare 4EA molecule product distributions, the cluster binding energy E_0 and the energy E_v of the chromophore vibrational state to be populated must be found. The only populated chromophore vibrations observed following 4EA(N₂)₁ and (CH₄)₁ excitation are those which show a $12 \text{ cm}^{-1} \Delta v = 0$ sequence structure at the bare 4EA molecule origin. As mentioned above, only the excited state/ground state energy difference is known for this mode (sequence structure), not an absolute value for its energy in either electronic state. Therefore, the 4EA(CH₄)₁ cluster results (rates and bare molecule sequence band intensities) are employed to obtain E_0 for this cluster (580 cm^{-1}) and E_v for the populated ethyl torsion vibration (35 cm^{-1}). The 4EA(N₂)₁ cluster data are fit assuming that the binding energy would be higher than that for 4EA(CH₄)₁ in analogy with the aniline cluster results.^{3(a),3(b)} The difference between the N₂ and the CH₄ cluster binding energies is 35 cm^{-1} for aniline, and since the binding energies are higher for 4EA, we choose 630 cm^{-1} for the 4EA(N₂)₁ cluster binding energy.

The results of the rate and product distribution calculations are presented in Table IV. The predictions of the model are quite good—less than 30% error for all observations for the 4EA(N₂)₁ and 4EA(CH₄)₁ clusters. The effect of uncertainties in the binding energy on the calculated rates is most severe for the low E^+ states. For example, adjustment of E_0 to 620 cm^{-1} for the N₂ cluster increases the calculated intensity for the $v' = 2$ state of the populated vibration following \bar{I}^2 excitation by 60%. The calculated VP rate from the vibrationless chromophore state of 4EA(N₂)₁ following \bar{I}^1 excitation changes by only 15%. Of course the relative error on the weaker high v' emissions is greater and therefore the required accuracy of the calculations is less for these peaks. The uncertainty in E_0 as determined by this method is $\pm 20 \text{ cm}^{-1}$, while the

TABLE IV. Comparison of calculated VP rates and product state intensities with experimental results.

Pumped state and observable	Solute and binding energy CH ₄ (580 cm ⁻¹)		N ₂ (630 cm ⁻¹)	
	Calculated	Observed	Calculated	Observed
\bar{I}^2				
Total rate (s ⁻¹)	2.8 × 10 ⁹	2.5 × 10 ⁹	2.3 × 10 ⁹	1.7 × 10 ⁹
Relative intensity				
<i>v</i> =0	1	1	1	1
<i>v</i> =1	0.46	0.38	0.40	0.21
<i>v</i> =2	0.19	0.11	0.10	0.06
<i>v</i> =3	0.06	0.029
\bar{I}^1				
Total rate (s ⁻¹)	5.8 × 10 ⁹	9.1 × 10 ⁹	5.5 × 10 ⁹	7.9 × 10 ⁹
Relative intensity				
<i>v</i> =0	1	1	1	1
<i>v</i> =1	0.56	0.51	0.56	0.50
<i>v</i> =2	0.31	0.26	0.27	0.22
<i>v</i> =3	0.14	0.13	0.10	0.12
<i>v</i> =4	0.06	0.076

uncertainty in the frequency of the populated (ethyl torsion) vibration is ± 5 cm⁻¹.

VI. DISCUSSION

At first glance, the emission spectra of 4EA following excitation of the N₂ and CH₄ clusters might appear to be due to some special propensity for dissociation from a particular vibrational mode of 4EA; however, all of the observed data can be reproduced by a statistical approach to VP. Systems for which IVR is fast compared to VP should maintain an equilibrium distribution among the low energy van der Waals and chromophore modes. Comparison of the calculated and observed product state distributions in Table IV shows that this expectation is borne out for 4EA(polyatomic solvent)₁ clusters. The "special mode" (35 cm⁻¹) is observed because of its extremely low energy. A low energy mode has a high probability of being populated since the system has a high density of states even with population in that mode. Furthermore, the VP rate suffers only a small decrease as quanta are left in the low frequency mode. The model also correctly predicts very little population in the 84 cm⁻¹ mode in these clusters.

Quantitative agreement can be obtained for the polyatomic solvent clusters, but not for the 4EA(Ar)₁ cluster. While the dispersed emission spectra of 4EA(Ar)₁ clusters are not sufficiently well resolved to allow quantitative measurement of product state distributions, the model predicts that the 4EA 0₀⁰ transition (at 0 cm⁻¹ in Fig. 2) should be the most intense feature in the emission if IVR can establish an equilibrium population distribution within the clusters prior to VP. Clearly this is not the case for 4EA(Ar)₁. This is almost surely due to breakdown of the assumption that all IVR is fast compared to VP. This can be clearly seen from Tables II and IV. The IVR time in the N₂ and

CH₄ clusters following $\bar{6a}^1$ excitation is $\lesssim 100$ ps (Table II), and is probably faster following \bar{I}^2 or \bar{I}^1 excitation due to the increased density of states at these high vibrational energies. The slower product (0₀⁰) rise times following \bar{I}^2 or \bar{I}^1 excitation of N₂ and CH₄ clusters are therefore determined by the VP time, and good agreement between the calculated and observed rates is obtained (Table IV). The kinetics of the 4EA(Ar)₁ cluster are quite different. Slow IVR (200 ps) is obtained following $\bar{6a}^1$ excitation. Calculated VP times for \bar{I}^2 or \bar{I}^1 excitation are roughly 10–20 ps. Product state rise times for \bar{I}^2 and \bar{I}^1 excitations are comparable to the $\bar{6a}^1$ IVR time of 200 ps, however, indicating that the dissociation process in 4EA(Ar)₁ is always limited by the IVR rate. Nonetheless the model does predict several of the qualitative trends in the 4EA(Ar)₁ data. The calculations predict that the VP rates decrease much less quickly with vibrational energy left in the 4EA molecule for Ar than for polyatomic solvents. For example, at approximately 175 cm⁻¹ of energy restricted to 4EA vibrations (five quanta of the ethyl torsion), the VP rates for N₂ and CH₄ clusters decrease by a factor of 15–20 as compared to a factor of 3 for the Ar cluster. This would result in far more intensity in the higher overtone sequence structure of 4EA(Ar)₁ as is observed. The presence of fewer van der Waals modes in the Ar cluster results in the prediction that the higher energy 84 cm⁻¹ ethyl bend mode would be significantly populated. In agreement with this prediction, at least one member of the 16 cm⁻¹ progression is observed.

IVR may populate several different chromophore states with sufficient energy in the van der Waals modes that VP can occur. If VP, which is predicted to be very fast in the Ar cluster, competes with subsequent IVR, then these chromophore states will be populated in the bare molecule. This would give a more crowded spectrum with greater intensity away from the 0₀⁰ transition as is observed. These predictions are in qualitative agreement with all cluster data; however, quantitative comparison for the Ar cluster is rendered impossible by crowding of the spectra (see Fig. 2).

The VP rate and product state emission intensity calculations are performed for several sets of van der Waals vibrational frequencies in order to test the sensitivity of the model to these frequencies. An increase of the van der Waals frequencies of 30% for the 4EA(CH₄)₁ results in a 20% increase in the VP rates for \bar{I}^2 excitation and a 30% increase in calculated rates for \bar{I}^1 excitation. The equilibrated cluster state distributions are affected little by these changes in mode energies (<10%). In fact, since P_v is calculated at high energy (E and $E-E_v$) for which the density of states is large, one can even use the classical (Marcus–Rice) approximation for density of states.¹⁷ Calculation of P_v [Eq. (2)] requires a ratio of densities of states at similar energies which leads to a cancellation of errors. The calculation of VP rates is somewhat more sensitive to the exact values of the mode energies as stated above, since the density of states in the denominator of Eq. (1) is calculated at high energy ($E-E_v$), while the sum of

states in the numerator is calculated at an energy above the binding energy (E^+) which can be quite small. At low energies, the sensitivity of the calculation to van der Waals mode frequency is greater. The sum of states is not a smooth function at low energies and the energies at which it exhibits a high degree of structure is a function of the vibrational frequencies.

Correcting for anharmonicity in the van der Waals modes is not simple because some modes change to free rotor modes at high energy. In addition, modes begin to mix significantly even at low excitation energy. Correcting all modes for a 3% anharmonicity ($\nu_{1-2}/\nu_{0-1} \sim 0.96$) changes the VP rate constants by about a factor of 3. Considering uncertainties involved in the corrections and partial cancellation of the effect in the final rates, we have chosen to ignore anharmonicity corrections for polyatomic solvent clusters. A 3% correction is employed, however, for the translational modes of the 4EA(Ar)₁ cluster.

VII. CONCLUSIONS

The IVR/VP dynamics of 4-ethylaniline clustered with argon, nitrogen, and methane have been observed and characterized by dispersed emission and time-resolved spectroscopy. The data include both overall rate constants for the processes and final state vibration distributions for the bare 4-ethylaniline chromophore. All low energy vibrational modes (both van der Waals and chromophore) comprise the phase space for consideration of the RRKM theory of the unimolecular vibrational predissociation reaction. Final product state distributions for the 4-ethylaniline chromophore following VP depend only on the competitive IVR and VP rates and the energy of the chromophore mode. The only chromophore mode found to be important for this final state distribution is the ~ 35 cm⁻¹ excited state ethyl torsion. Its importance as a final product state arises solely from its low energy. For the 4EA(Ar)₁ cluster, the condition that $k_{VP} \ll k_{IVR}$ is not met and the vibrational population of the cluster does not reflect an internal equilibrium distribution of cluster vibrational energy between the van der Waals modes and the chromophore modes. For the 4EA (polyatomic solvent)₁ clusters, $k_{VP} \ll k_{IVR}$ and an internal equilibrium between the vibrational cluster modes is established and the relative intensities of the $\Delta v=0$ torsional sequence bands of the chromophore following IVR/VP can be calculated accu-

rately. A statistical sequential IVR/VP model readily explains (both qualitatively and quantitatively) the entire data set of rates, intensities, and final product state distributions for these 4EA/solvent clusters. The rate calculations are not particularly sensitive to the van der Waals mode energies used, but do depend on the values of the anharmonicities chosen for the modes.

ACKNOWLEDGMENTS

The authors wish to thank Dr. Robert Disselkamp for performing the *ab initio* calculations for 4-ethylaniline. This work was supported by the NSF.

- ¹J. A. Beswick and J. Jortner, *J. Chem. Phys.* **68**, 2277 (1978).
- ²(a) D. V. Brumbaugh, J. E. Kenny, and D. H. Levy, *J. Chem. Phys.* **78**, 3415 (1983); (b) D. L. Osborn, J. C. Alfano, N. van Dantzig, and D. H. Levy, *ibid.* **97**, 2276 (1992); (c) J. C. Alfano, S. J. Martinez, and D. H. Levy, *ibid.* **94**, 1673 (1991); (d) *J. Mol. Spectrosc.* **143**, 366 (1990).
- ³(a) M. R. Nimlos, M. A. Young, E. R. Bernstein, and D. F. Kelley, *J. Chem. Phys.* **91**, 5268 (1988); (b) M. F. Hineman, S. K. Kim, E. R. Bernstein, and D. F. Kelley, *ibid.* **96**, 4904 (1992); (c) D. F. Kelley and E. R. Bernstein, *J. Phys. Chem.* **90**, 5164 (1986); (d) E. A. Outhouse, G. A. Bickel, D. R. Dremmer, and S. C. Wallace, *J. Chem. Phys.* **95**, 6261 (1991).
- ⁴J. L. Knee, L. R. Khundkar, and A. H. Zewail, *J. Chem. Phys.* **87**, 115 (1987).
- ⁵P. M. Felker and A. H. Zewail, *Adv. Chem. Phys.* **70**, 265 (1988).
- ⁶D. E. Powers, J. B. Hopkins, and R. E. Smalley, *J. Chem. Phys.* **72**, 5721 (1980).
- ⁷(a) J. B. Hopkins, D. E. Powers, and R. E. Smalley, *J. Chem. Phys.* **72**, 5039 (1980); (b) J. B. Hopkins, D. E. Powers, S. Mukamel, and R. E. Smalley, *ibid.* **72**, 5049 (1980); (c) J. B. Hopkins, D. E. Powers, and R. E. Smalley, *ibid.* **73**, 683 (1980).
- ⁸J. B. Hopkins, D. E. Powers, and R. E. Smalley, *J. Chem. Phys.* **74**, 745 (1981).
- ⁹E. R. Bernstein, K. Law, and M. Schauer, *J. Chem. Phys.* **80**, 634 (1984).
- ¹⁰S. Li and E. R. Bernstein, *J. Chem. Phys.* **95**, 1577 (1991).
- ¹¹R. Disselkamp and E. R. Bernstein, *J. Chem. Phys.* (to be published).
- ¹²(a) S. L. Mayo, B. D. Olafson, and W. A. Goddard III, *J. Phys. Chem.* **94**, 8897 (1990); (b) N. Karasawa, S. Dasgupta, and W. A. Goddard III, *ibid.* **95**, 2260 (1991).
- ¹³M. Dupuis and A. Farazdel, *HONDO* (IBM Corp., Center for Scientific & Engineering Computations, Kingston, New York, 1990).
- ¹⁴J. J. P. Stewart, *MOPAC, A General Molecular Orbital Package*, 6th ed. (F. I. S. Eiler Research Laboratory, USAF, Colorado Springs, CO, 1990).
- ¹⁵R. Disselkamp and E. R. Bernstein, *J. Chem. Phys.* (to be published).
- ¹⁶M. F. Hineman, G. A. Bruker, D. F. Kelley, and E. R. Bernstein, *J. Chem. Phys.* **97**, 3341 (1992).
- ¹⁷P. J. Robinson and K. A. Holbrook, *Unimolecular Reactions* (Wiley, New York, 1972).